Published in Journal of Quantitative Spectroscopy and Radiative Transfer 221 (2018) 260 - 272

Co-Polarized and Cross-Polarized Scattering of an Off-Axis Focused Gaussian Beam by a Spherical Particle. 1. Exact GLMT Formalism

James A. Lock[1,*] and Philip Laven[2]
[1] Physics Dept., Cleveland State University, Cleveland, OH 44115, USA
[2] 9 Russells Crescent, Horley RH6 7DJ, UK
[*] Corresponding author. *E-mail address:* j.lock@csuohio.edu

Abstract
In static and dynamic light scattering, it has frequently been claimed that cross-polarized scattering cannot occur for single-scattering by a homogeneous spherical particle. Although this is true for both plane wave and on-axis Gaussian beam incidence, we show that cross-polarized scattering does occur when the beam is translated off-axis incidence perpendicular to the scattering plane. We find that the existence of cross-polarized scattering is a direct result of the breaking of the circular symmetry of the beam with respect to the center of the particle when the beam is translated off-axis in wave theory, and to the constraint of the incident beam being a solution of Maxwell's equations.

Key words: Mie theory, generalized Lorenz-Mie theory, polarization-resolved scattering, cross-polarized scattering

1. Introduction

In static and dynamic light scattering experiments, a large number of scattering particles are suspended in a liquid-filled sample cell and are illuminated by an incident beam traveling in the horizontal $+z$ direction. The scattering plane is taken to be the horizontal yz plane of a Cartesian coordinate system, and the x axis is vertical. The beam is linearly polarized either perpendicular to the horizontal scattering plane (i.e. vertically or V) or in the scattering plane (i.e. horizontally or H) [1-3]. Light scattered by the particles passes through a polarizer oriented either vertically (V) or horizontally (H) before being recorded by a detector, as is shown in Fig. 1. In the context of static and dynamic light scattering, it is frequently claimed that if the scattering particles are homogeneous spheres and only single-scattering occurs in the sample cell, then co-polarized VV and HH scattering is observed, but cross-polarized VH and HV scattering cannot occur. If VH or HV scattering is experimentally detected under such conditions, it is commonly taken to be a sign that the scattering particles are either (i) anisotropic [1], (ii) non-spherical [4,5], or (iii) that the number density of particles in the sample cell is sufficiently large so that multiple scattering is occurring [6].

The reason for this claim is understandable. The polarization state of light scattered by a target particle is connected to the polarization state of a plane wave incident on it by the 2×2 scattering amplitude matrix [**S**] (see p.34 of [7], Eq.(3.12) of [8], and Eq.(2.30) of [9]). The four elements of [**S**] describe VV, VH, HV, and HH scattering. It has long been known that if the target particle is a homogeneous sphere and an incident plane wave propagates in the z direction toward the target, then the scattering amplitude matrix is diagonal, i.e. $S_{VH}=S_{HV}=0$, and only co-polarized scattering occurs (see p.56 of [3]). Since the macromolecules or small particles frequently studied in dynamic light scattering experiments are sub-micron in size, the phase fronts of an incident beam are nearly flat across their diameter. As a result, plane wave incidence is a good approximation to this situation, even if the incident fields are those of a moderately focused laser beam. But since the fields of a transversely focused beam can be expanded as an angular spectrum of plane waves (see Sec.3.7 of [10] and [11]), and each diagonally incident component wave in the spectrum gives rise to a nonzero S_{VH} and S_{HV} (see Eqs.(5.145)-(5.148) of [9]), it is sensible to conjecture that cross-polarized scattering should be able to occur, and might possibly be experimentally detectable under very favorable conditions. The purpose of this study is to consider the case of a transversely focused beam incident on a single homogeneous spherical particle, and the conditions under which cross-polarized scattering occurs.

Published in Journal of Quantitative Spectroscopy and Radiative Transfer 221 (2018) 260 - 272

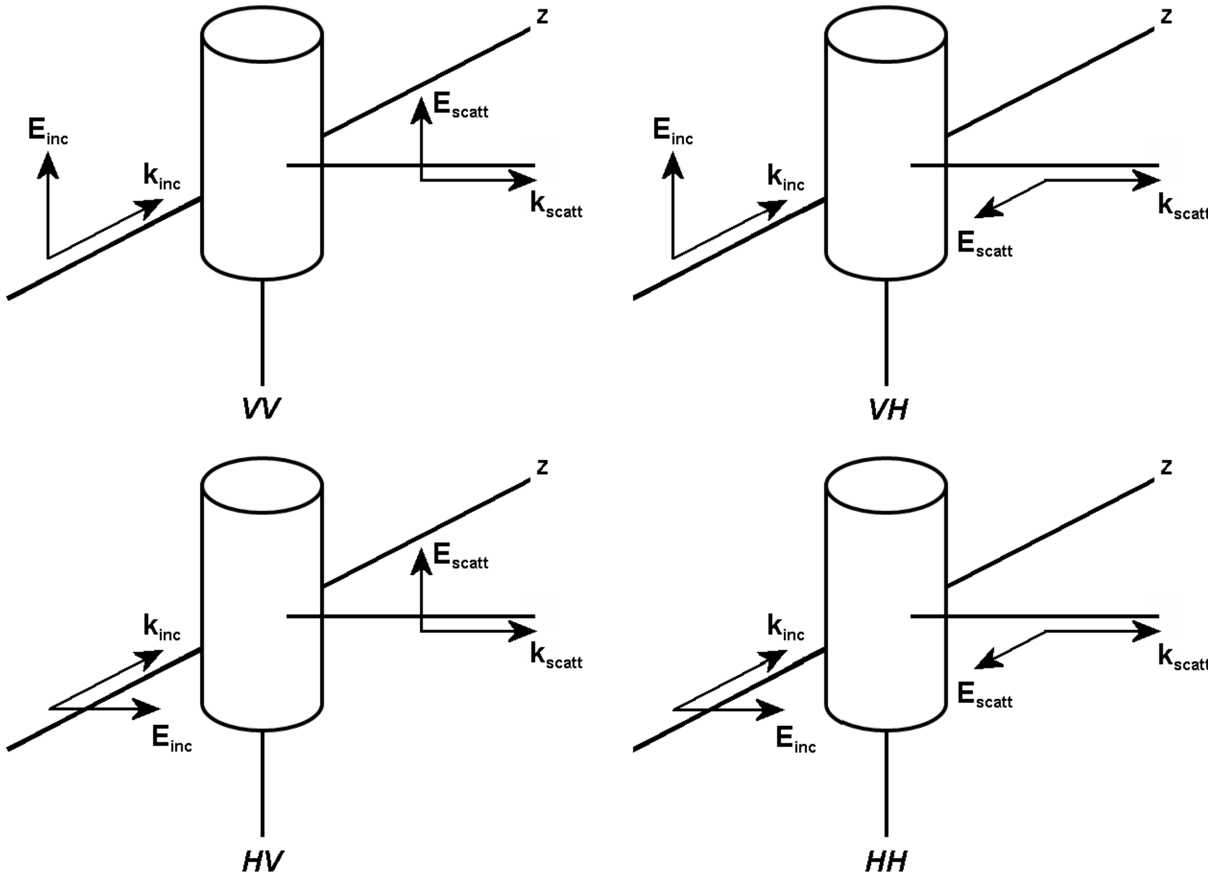

Fig. 1: Geometry of VV, VH, HV, and HH scattering.

The body of this study proceeds as follows. In Section 2 the generalized Lorenz-Mie theory (GLMT) formulas for scattering of an arbitrary transversely focused beam by a spherical particle are reviewed. The incident beam is then taken to be the localized model of a focused Gaussian beam that is polarized at the center of its focal waist either in the scattering plane or perpendicular to it. In Section 3, a numerical example is then presented which exhibits both co-polarized and cross-polarized scattering for off-axis incidence of the beam with respect to the target particle. In Section 4 the existence of non-zero cross-polarized scattering is seen to be a wave theory effect due to the breaking of circular symmetry of the beam with respect to the particle when the beam is translated off-axis, and to the fact that the off-axis beam fields are a solution to Maxwell's equations. As is seen in Sec.2, the GLMT formulas for the scattering amplitudes for off-axis beam incidence contain sums over both partial waves and azimuthal modes. In Part 2 of this study [12] the GLMT angular functions are accurately approximated for large partial waves. This allows the sum over azimuthal modes to be evaluated analytically, leaving only the sum over partial waves to be evaluated numerically, as is also the case for Lorenz-Mie scattering of a plane wave.

2. Off-Axis Scattering by the Localized Model of a Focused Gaussian Beam

2a. Generalized Lorenz-Mie Theory

Scattering of an incident monochromatic transversely focused beam of nominal electric field strength E_0, wavelength λ, wave number $k=2\pi/\lambda$, and angular frequency ω by a homogeneous spherical particle of radius a and refractive index M is calculated here using the GLMT formalism. The $r\to\infty$ far-zone scattered electric and magnetic fields are

Published in Journal of Quantitative Spectroscopy and Radiative Transfer 221 (2018) 260 - 272

$$\mathbf{E}_{\mathbf{scatt}}(r,\theta,\varphi) = (\mathrm{i}E_0/kr)\exp(\mathrm{i}kr)\,[S_2(\theta,\varphi)\,\mathbf{u}_\theta - S_1(\theta,\varphi)\,\mathbf{u}_\varphi] \tag{1a}$$

$$\mathbf{B}_{\mathbf{scatt}}(r,\theta,\varphi) = (\mathrm{i}E_0/ckr)\exp(\mathrm{i}kr)\,[S_1(\theta,\varphi)\,\mathbf{u}_\theta + S_2(\theta,\varphi)\,\mathbf{u}_\varphi]\ , \tag{1b}$$

where φ is the azimuthal angle with respect to the xz plane, θ is the scattering angle, c is the speed of light, and the time dependence exp(-iωt) has been left implicit. The horizontal scattering plane considered in the numerical example of Sec. 3 is $\varphi=\pm 90°$. If one considers scattering in a plane corresponding to a fixed value of φ, then $\mathbf{u}_\mathbf{r}$ and $\mathbf{u}_\theta$ are orthogonal unit vectors in that plane, and $\mathbf{u}_\varphi$ is the unit vector perpendicular to that plane. In the notation of [13,14], (but with $A_{nm}^{\pm}$ and $B_{nm}^{\pm}$ defined in Eqs.(3a),(3b) below rather than by Eq.(48) of [13]), the scattering amplitudes are

$$\begin{aligned} S_1(\theta,\varphi) = \sum_{n=1}^{\infty} c_n \{ &(1/2)\, B_n^{\,0}\, b_n\, \tau_n^{\,0}(\theta) \\ &+ \sum_{m=1}^{n} [B_{nm}^{\,+}\, b_n\, \tau_n^{\,m}(\theta)\cos(m\varphi) + \mathrm{i}\, B_{nm}^{\,-}\, b_n\, \tau_n^{\,m}(\theta)\sin(m\varphi) \\ &\quad + A_{nm}^{\,+}\, a_n\, m\pi_n^{\,m}(\theta)\sin(m\varphi) - \mathrm{i}\, A_{nm}^{\,-}\, a_n\, m\pi_n^{\,m}(\theta)\cos(m\varphi)]\}\ , \end{aligned} \tag{2a}$$

$$\begin{aligned} S_2(\theta,\varphi) = \sum_{n=1}^{\infty} c_n \{ &(1/2)\, A_n^{\,0}\, a_n\, \tau_n^{\,0}(\theta) \\ &+ \sum_{m=1}^{n} [A_{nm}^{\,+}\, a_n\, \tau_n^{\,m}(\theta)\cos(m\varphi) + \mathrm{i}\, A_{nm}^{\,-}\, a_n\, \tau_n^{\,m}(\theta)\sin(m\varphi) \\ &\quad - B_{nm}^{\,+}\, b_n\, m\pi_n^{\,m}(\theta)\sin(m\varphi) + \mathrm{i}\, B_{nm}^{\,-}\, b_n\, m\pi_n^{\,m}(\theta)\cos(m\varphi)]\}\ . \end{aligned} \tag{2b}$$

where

$$A_{nm}^{\pm} \equiv (1/2)\,(A_n^{\,m} \pm A_n^{\,-m}) \text{ for } 1 \le m \le n \tag{3a}$$

$$B_{nm}^{\pm} \equiv (1/2)\,(B_n^{\,m} \pm B_n^{\,-m}) \text{ for } 1 \le m \le n\ . \tag{3b}$$

The quantities $A_n^{\,m}$, $B_n^{\,m}$ are the beam shape coefficients of the incident beam for partial wave numbers $1 \le n < \infty$ and azimuthal modes $-n \le m \le n$. If the radial component of the incident electric and magnetic fields is exactly known, the beam shape coefficients may be obtained from [13,14]

$$\begin{aligned} A_n^{\,m} = &[(-\mathrm{i})^{n-1}/2\pi]\,[kr/j_n(kr)]\,[(n-|m|)!/(n+|m|)!] \\ &\times \int_0^{\pi} \sin(\theta)\,\mathrm{d}\theta \int_0^{2\pi} \mathrm{d}\varphi\ \mathrm{P}_n^{\,|m|}[\cos(\theta)]\,\exp(-\mathrm{i}m\varphi)\, E_{inc}^{\ rad}(r,\theta,\varphi) \end{aligned} \tag{4a}$$

$$\begin{aligned} B_n^{\,m} = &[(-\mathrm{i})^{n-1}/2\pi]\,[kr/j_n(kr)]\,[(n-|m|)!/(n+|m|)!] \\ &\times \int_0^{\pi} \sin(\theta)\,\mathrm{d}\theta \int_0^{2\pi} \mathrm{d}\varphi\ \mathrm{P}_n^{\,|m|}[\cos(\theta)]\,\exp(-\mathrm{i}m\varphi)\, cB_{inc}^{\ rad}(r,\theta,\varphi)\ , \end{aligned} \tag{4b}$$

where $j_n(kr)$ is a spherical Bessel function. If $E_{inc}^{\ rad}(r,\theta,\varphi)$ and $B_{inc}^{\ rad}(r,\theta,\varphi)$ are the radial field components of an exact solution of Maxwell's equations, the integrals over θ and φ will exactly cancel the $[kr/j_n(kr)]$ term, and produce coordinate-independent values of $A_n^{\,m}$ and $B_n^{\,m}$. The beam shape coefficients for n,m and $n,-m$ in Eqs.(2a),(2b) have been combined as Eqs.(3a),(3b) in order to take advantage of certain simplifications that analytically and numerically occur when summing over only non-negative values of m.

Published in Journal of Quantitative Spectroscopy and Radiative Transfer 221 (2018) 260 - 272

In Eqs.(2a),(2b), the transverse magnetic (TM) and transverse electric (TE) partial wave scattering amplitudes of Lorenz-Mie theory are a_n, b_n, respectively (see p.123 of [7] and Eqs.(4.56),(4.57) of [8]), and the GLMT angular functions are

$$m\pi_n^{m}(\theta) = [m/\sin(\theta)]\ \mathrm{P}_n^{m}[\cos(\theta)] \tag{5a}$$
$$\tau_n^{m}(\theta) = \mathrm{d}\mathrm{P}_n^{m}[\cos(\theta)]\ /\ \mathrm{d}\theta\ , \tag{5b}$$

where $\mathrm{P}_n^{m}[\cos(\theta)]$ are associated Legendre functions as defined in Eqs.(12.81),(12.81a) of [15]. The Lorenz-Mie partial wave weighting coefficient in Eqs.(2a),(2b) is

$$c_n = (2n+1)/[n(n+1)]\ . \tag{6}$$

It should be noted that another notation for the beam shape coefficients uses $g_n^{m}{}_{TM}$ rather than A_n^{m} and $g_n^{m}{}_{TE}$ rather than B_n^{m} [16,17]. Correcting for the different conventions for the time dependence of the fields, the spherical Hankel functions used [18], and the different scaling factor of the associated Legendre functions, one has $A_n^{m} = 2g_n^{m}{}_{TM}$ and $B_n^{m}=2g_n^{m}{}_{TE}$.

2b. Localized Model Beam Shape Coefficients and Scattering Amplitudes

The calculations reported here use the localized model of an off-axis focused Gaussian beam propagating in the $+z$ direction and linearly polarized in the x direction at the center of its focal waist. After preliminary partial reports, the shape coefficients of this beam type were first fully published in [19]. A simplified form for them was obtained in [14], they were related to Davis beams in [20], and they were derived using angular spectrum of plane waves method in [11,21]. Useful reviews of the localized beam model are given in [22,23]. A localized beam is by definition an exact solution of Maxwell's equations since its beam shape coefficients are constants, and its electric field profile has been found to be very nearly Gaussian as long as the beam width at the center of its focal waist is more than a few wavelengths [19,24-29]. It has been found that as this exact beam is progressively translated off-axis on the φ_0 direction, a very weak secondary Gaussian peak starts to form that is translated equally far in the φ_0+180° direction. This secondary peak is sufficiently weak that it should not affect the numerical results obtained in Sec.3 [19,26-29].

The localized beam is parameterized by the confinement parameter

$$s = \lambda/(2\pi w_0)\ , \tag{7}$$

where w_0 is the electric field half-width of the beam at the center of its focal waist. For the calculations described here, the beam is focused on the scattering particle, rather than upstream or downstream from it. The center of the scattering particle coincides with the origin of the transverse plane containing the center of the beam's focal waist at the point (ρ_0,φ_0) given in polar coordinates. When ρ_0=0, the beam is said to be on-axis with respect to the particle, and when $\rho_0 \neq 0$, it is said to be off-axis. The angle φ_0 describes the direction in which the beam is translated off-axis and is not to be confused with the orientation of the scattering plane which is parameterized by the azimuthal angle φ. If the electric field of an incident focused Gaussian beam is polarized in the $\mathbf{u_x}$ direction at the center of the focal waist, the localized model beam shape coefficients in the notation of [13,14], are

$$A_{nm}^{+}(\rho_0,\varphi_0) = \mathrm{i}\ F_n\ (n+1/2)\ [-\ \mathrm{i}/(n+1/2)]^{m} \times \{\mathrm{I}_{m-1}(Q_n) \cos[(m-1)\varphi_0] + \mathrm{I}_{m+1}(Q_n)\ \cos[(m+1)\varphi_0]\} \tag{8a}$$

$$A_{nm}^{-}(\rho_0,\varphi_0) = F_n\ (n+1/2)\ [-\ \mathrm{i}/(n+1/2)]^{m} \times \{\mathrm{I}_{m-1}(Q_n)\ \sin[(m-1)\varphi_0] + \mathrm{I}_{m+1}(Q_n)\ \sin[(m+1)\varphi_0]\} \tag{8b}$$

$$A_n^{0}(\rho_0,\varphi_0) = 2\mathrm{i}\ F_n\ (n+1/2)\ \mathrm{I}_1(Q_n)\ \cos(\varphi_0) \tag{8c}$$

and

Published in Journal of Quantitative Spectroscopy and Radiative Transfer 221 (2018) 260 - 272

$$B_{nm}^{+}(\rho_0,\varphi_0) = -\mathrm{i}\, F_n\, (n+1/2)\, [-\,\mathrm{i}/(n+1/2)]^m \times \{\mathrm{I}_{m-1}(Q_n)\, \sin[(m-1)\varphi_0] - \mathrm{I}_{m+1}(Q_n)\, \sin[(m+1)\varphi_0]\} \quad (9a)$$

$$B_{nm}^{-}(\rho_0,\varphi_0) = F_n\, (n+1/2)\, [-\,\mathrm{i}/(n+1/2)]^m \times \{\mathrm{I}_{m-1}(Q_n)\, \cos[(m-1)\varphi_0] - \mathrm{I}_{m+1}(Q_n)\, \cos[(m+1)\varphi_0]\} \quad (9b)$$

$$B_n^{0}(\rho_0,\varphi_0) = 2\mathrm{i}\, F_n\, (n+1/2)\, \mathrm{I}_1(Q_n)\, \sin(\varphi_0)\ , \quad (9c)$$

where

$$F_n \equiv \exp(-\rho_0^2/w_0^2)\, \exp[-s^2\, (n+1/2)^2] \quad (10)$$
$$Q_n \equiv (2s\rho_0/w_0)\, (n+1/2)\ , \quad (11)$$

and $\mathrm{I}_m(Q_n)$ is a modified Bessel function. In the limit $\rho_0 \to 0$ and $Q_n \to 0$, one obtains $F_n \to \exp[-s^2(n+1/2)^2]$, which is proportional to the $m=\pm1$ beam shape coefficients of an on-axis focused Gaussian beam ([24,25,30,31] and Eq.(VII.7) of [17]). In the limit $s \to 0$ and $Q_n \to 0$, one obtains $F_n \to 1$, which is proportional to the $m=\pm1$ beam shape coefficients of a plane wave (see Eqs.(VI.78),(VI.79) of [17]).

If the electric field at the center of the focal waist is instead polarized in the $\mathbf{u}_y$ direction, using the angular spectrum of plane waves procedure outlined in [21], we found that the beam shape coefficients are

$$A_{nm}^{+}(\rho_0,\varphi_0) = -\mathrm{i}\, F_n\, (n+1/2)\, [-\,\mathrm{i}/(n+1/2)]^m \times \{\mathrm{I}_{m-1}(Q_n)\, \sin[(m-1)\varphi_0] - \mathrm{I}_{m+1}(Q_n)\, \sin[(m+1)\varphi_0]\} \quad (12a)$$

$$A_{nm}^{-}(\rho_0,\varphi_0) = F_n\, (n+1/2)\, [-\,\mathrm{i}/(n+1/2)]^m \times \{\mathrm{I}_{m-1}(Q_n)\, \cos[(m-1)\varphi_0] - \mathrm{I}_{m+1}(Q_n)\, \cos[(m+1)\varphi_0]\} \quad (12b)$$

$$A_n^{0}(\rho_0,\varphi_0) = 2\mathrm{i}\, F_n\, (n+1/2)\, \mathrm{I}_1(Q_n)\, \sin(\varphi_0) \quad (12c)$$

and

$$B_{nm}^{+}(\rho_0,\varphi_0) = -\mathrm{i}F_n\, (n+1/2)\, [-\,\mathrm{i}/(n+1/2)]^m \times \{\mathrm{I}_{m-1}(Q_n)\, \cos[(m-1)\varphi_0] + \mathrm{I}_{m+1}(Q_n)\, \cos[(m+1)\varphi_0]\} \quad (13a)$$

$$B_{nm}^{-}(\rho_0,\varphi_0) = -\, F_n\, (n+1/2)\, [-\,\mathrm{i}/(n+1/2)]^m \times \{\mathrm{I}_{m-1}(Q_n)\, \sin[(m-1)\varphi_0] + \mathrm{I}_{m+1}(Q_n)\, \sin[(m+1)\varphi_0]\} \quad (13b)$$

$$B_n^{0}(\rho_0,\varphi_0) = -2\mathrm{i}\, F_n\, (n+1/2)\, \mathrm{I}_1(Q_n)\, \cos(\varphi_0)\ . \quad (13c)$$

To the best of our knowledge, the beam shape coefficients for a *y*-polarized localized model off-axis Gaussian beam have not appeared in this form in the literature before. Equivalent results, though expressed rather differently, and based on rotating an *x*-polarized beam and the scattering plane by 90° while leaving the Cartesian axes fixed, were derived in [32,33]. The beam shape coefficients satisfy a number of symmetry relations. In particular, A_{nm}^{+}, A_{nm}^{-}, A_n^{0} for a *y*-polarized beam are the same as B_{nm}^{+}, B_{nm}^{-}, B_n^{0} for an *x*-polarized beam, and B_{nm}^{+}, B_{nm}^{-}, B_n^{0} for a *y*-polarized beam are the negative of A_{nm}^{+}, A_{nm}^{-}, A_n^{0} for an *x*-polarized beam. The beam shape coefficients for a localized off-axis Gaussian beam linearly polarized in any transverse direction can be written as a linear combination of the coefficients of an *x*-polarized and a *y*-polarized beam.

When the electric field of the incident beam is *x*-polarized at the center of its focal waist, substitution of Eqs.(8),(9) for the localized beam shape coefficients into Eqs.(2a),(2b) for the scattering amplitudes gives

Published in Journal of Quantitative Spectroscopy and Radiative Transfer 221 (2018) 260 - 272

$$S_1(\theta,\varphi;\rho_0,\varphi_0) = \mathrm{i} \sum_{n=1}^{\infty} c_n\, F_n\, (n+1/2)\, b_n\, \mathrm{I}_1(Q_n)\, \tau_n^{\,0}(\theta)\, \sin(\varphi_0)$$

$$+ \mathrm{i} \sum_{n=1}^{\infty} c_n\, F_n\, (n+1/2)\, b_n \sum_{m=1}^{n} [\text{-}\mathrm{i}/(n+1/2)]^m\, \tau_n^{\,m}(\theta)$$

$$\times [\mathrm{I}_m^{\,-}(Q_n) \sin(m\chi) \cos(\varphi_0) + \mathrm{I}_m^{\,+}(Q_n) \cos(m\chi) \sin(\varphi_0)]$$

$$+ \mathrm{i} \sum_{n=1}^{\infty} c_n\, F_n\, (n+1/2)\, a_n \sum_{m=1}^{n} [\text{-}\mathrm{i}/(n+1/2)]^m\, m\pi_n^{\,m}(\theta)$$

$$\times [\mathrm{I}_m^{\,+}(Q_n) \sin(m\chi) \cos(\varphi_0) + \mathrm{I}_m^{\,-}(Q_n) \cos(m\chi) \sin(\varphi_0)] \qquad (14a)$$

and

$$S_2(\theta,\varphi;\rho_0,\varphi_0) = \mathrm{i} \sum_{n=1}^{\infty} c_n\, F_n\, (n+1/2)\, a_n\, \mathrm{I}_1(Q_n)\, \tau_n^{\,0}(\theta)\, \cos(\varphi_0)$$

$$+ \mathrm{i} \sum_{n=1}^{\infty} c_n\, F_n\, (n+1/2)\, a_n \sum_{m=1}^{n} [\text{-}\mathrm{i}/(n+1/2)]^m\, \tau_n^{\,m}(\theta)$$

$$\times [\mathrm{I}_m^{\,+}(Q_n) \cos(m\chi) \cos(\varphi_0) - \mathrm{I}_m^{\,-}(Q_n) \sin(m\chi) \sin(\varphi_0)]$$

$$+ \mathrm{i} \sum_{n=1}^{\infty} c_n\, F_n\, (n+1/2)\, b_n \sum_{m=1}^{n} [\text{-}\mathrm{i}/(n+1/2)]^m\, m\pi_n^{\,m}(\theta)$$

$$\times [\mathrm{I}_m^{\,-}(Q_n) \cos(m\chi) \cos(\varphi_0) - \mathrm{I}_m^{\,+}(Q_n) \sin(m\chi) \sin(\varphi_0)] \;, \qquad (14b)$$

where

$$\mathrm{I}_m^{\,\pm}(Q_n) \equiv \mathrm{I}_{m-1}(Q_n) \pm \mathrm{I}_{m+1}(Q_n) \qquad (15)$$

$$\chi \equiv \varphi - \varphi_0 \;. \qquad (16)$$

When the electric field of the incident beam is y-polarized at the center of its focal waist, substitution of Eqs.(12),(13) into Eqs.(2a),(2b) gives

$$S_1(\theta,\varphi;\rho_0,\varphi_0) = -\mathrm{i} \sum_{n=1}^{\infty} c_n\, F_n\, (n+1/2)\, b_n\, \mathrm{I}_1(Q_n)\, \tau_n^{\,0}(\theta)\, \cos(\varphi_0)$$

$$- \mathrm{i} \sum_{n=1}^{\infty} c_n\, F_n\, (n+1/2)\, b_n \sum_{m=1}^{n} [\text{-}\mathrm{i}/(n+1/2)]^m\, \tau_n^{\,m}(\theta)$$

$$\times [\mathrm{I}_m^{\,+}(Q_n) \cos(m\chi) \cos(\varphi_0) - \mathrm{I}_m^{\,-}(Q_n) \sin(m\chi) \sin(\varphi_0)]$$

$$- \mathrm{i} \sum_{n=1}^{\infty} c_n\, F_n\, (n+1/2)\, a_n \sum_{m=1}^{n} [\text{-}\mathrm{i}/(n+1/2)]^m\, m\pi_n^{\,m}(\theta)$$

$$\times [\mathrm{I}_m^{\,-}(Q_n) \cos(m\chi) \cos(\varphi_0) - \mathrm{I}_m^{\,+}(Q_n) \sin(m\chi) \sin(\varphi_0)] \qquad (17a)$$

and

Published in Journal of Quantitative Spectroscopy and Radiative Transfer 221 (2018) 260 - 272

$$S_2(\theta,\varphi;\rho_0,\varphi_0) = \mathrm{i} \sum_{n=1}^{\infty} c_n\, F_n\, (n+1/2)\, a_n\, \mathrm{I}_1(Q_n)\, \tau_n^{\,0}(\theta)\, \sin(\varphi_0)$$

$$+ \mathrm{i} \sum_{n=1}^{\infty} c_n\, F_n\, (n+1/2)\, a_n \sum_{m=1}^{n} [-\mathrm{i}/(n+1/2)]^m\, \tau_n^{\,m}(\theta)$$

$$\times [\mathrm{I}_m^{\,-}(Q_n)\, \sin(m\chi)\, \cos(\varphi_0) + \mathrm{I}_m^{\,+}(Q_n)\, \cos(m\chi)\, \sin(\varphi_0)]$$

$$+ \mathrm{i} \sum_{n=1}^{\infty} c_n\, F_n\, (n+1/2)\, b_n \sum_{m=1}^{n} [-\mathrm{i}/(n+1/2)]^m\, m\pi_n^{\,m}(\theta)$$

$$\times [\mathrm{I}_m^{\,+}(Q_n)\, \sin(m\chi)\, \cos(\varphi_0) + \mathrm{I}_m^{\,-}(Q_n)\, \cos(m\chi)\, \sin(\varphi_0)] \quad . \qquad (17b)$$

It should be noted that the scattering amplitudes also satisfy a number of symmetry relations. In particular, S_2 for a y-polarized beam is identical to S_1 for an x-polarized beam with the Lorenz-Mie partial wave scattering amplitudes a_n and b_n interchanged. Similarly, S_1 for a y-polarized beam is the negative of S_2 for an x-polarized beam with a_n and b_n interchanged. Since the scattering plane in the dynamic light scattering experiments described in Sec.1 is the horizontal yz plane with $\varphi=\pm 90°$, if the incident beam is polarized in the vertical x direction, the VV scattering amplitude is $S_1(\theta,\varphi;\rho_0,\varphi_0)$ and the VH scattering amplitude is $S_2(\theta,\varphi;\rho_0,\varphi_0)$. If the incident beam is polarized in the horizontal y direction, the HV scattering amplitude is $S_1(\theta,\varphi;\rho_0,\varphi_0)$ and the HH scattering amplitude is $S_2(\theta,\varphi;\rho_0,\varphi_0)$.

Equations (14)-(17) show that if the beam is displaced an equal distance above or below the scattering plane (i.e. $\varphi_0=0°$ or 180°), each of the individual VV, VH, HV, and HH scattered intensities is the same in the scattering plane to either side of the forward direction (i.e. φ or $-\varphi$ for fixed θ) [34]. Similarly, each of the individual VV and HH scattered intensities is the same when the beam is displaced off-axis to the left in the scattering plane and the detector is to the right, as when the beam is displaced off-axis to the right in the scattering plane and the detector is to the left [34]. Substitution of $\rho_0\to 0$ for an on-axis beam or $s\to 0$ for an incident plane wave into Eqs.(14),(17) verifies that for these special cases, the cross-polarized VH and HV scattered intensities are identically zero, as mentioned in Sec.1 concerning the impossibility of cross-polarized scattering by a homogeneous spherical particle. The VH and HV intensities are also identically zero when the beam is displaced off-axis in the scattering plane. But when the beam is displaced off-axis perpendicular to the scattering plane, the cross-polarized VH and HV scattered intensities are nonzero, and are examined in detail in Sec.3.

2c. Simplification for $\theta=0°$ and $\theta=180°$

Evaluation of S_{VV}, S_{VH}, S_{HV}, and S_{HH} as described in the comments following Eqs.(14)-(17) requires that the sum over azimuthal modes m must be either analytically or numerically evaluated. An exception to this occurs for $\theta=0°,180°$ where the only nonzero contribution to the sum is the $m=1$ term. The value of the GLMT angular functions in the forward direction is

$$\tau_n^{\,\pm 1}(0°) = \pi_n^{\,\pm 1}(0°) = n(n+1)/2 \qquad (18a)$$

$$\tau_n^{\,\pm m}(0°) = \pi_n^{\,\pm m}(0°) = 0 \text{ for } m \neq 1 \quad . \qquad (18b)$$

For an x-polarized incident beam, substituting Eqs.(18a),(18b) into Eqs.(14a),(14b) gives

$$S_1(0°,\varphi;\rho_0,\varphi_0) = \sum_{n=1}^{\infty} F_n\, (n+1/2)\, (a_n+b_n)\, \mathrm{I}_0(Q_n)\, \sin(\varphi)$$

$$+ \sum_{n=1}^{\infty} F_n\, (n+1/2)\, (a_n-b_n)\, \mathrm{I}_2(Q_n)\, \sin(\varphi-2\varphi_0) \quad , \qquad (19a)$$

Published in Journal of Quantitative Spectroscopy and Radiative Transfer 221 (2018) 260 - 272

$$S_2(0°,\varphi;\rho_0,\varphi_0) = \sum_{n=1}^{\infty} F_n\,(n+1/2)\,(a_n+b_n)\,\mathrm{I}_0(Q_n)\cos(\varphi)$$

$$+ \sum_{n=1}^{\infty} F_n\,(n+1/2)\,(a_n-b_n)\,\mathrm{I}_2(Q_n)\cos(\varphi-2\varphi_0)\ . \qquad (19b)$$

Since φ is indeterminate when θ=0°, neither S_1 nor S_2 alone can correspond to the scattered electric field in the x or y direction. They must be combined together as in Eq.(1a) in order to cancel away the φ dependence. Evaluating $\mathbf{u_\theta}$ and $\mathbf{u_\varphi}$ at θ=0°, one obtains

$$\mathbf{u_\theta} = \cos(\varphi)\,\mathbf{u_x} + \sin(\varphi)\,\mathbf{u_y} \qquad (20a)$$

$$\mathbf{u_\varphi} = -\sin(\varphi)\,\mathbf{u_x} + \cos(\varphi)\,\mathbf{u_y}\ . \qquad (20b)$$

The forward-scattered electric field of Eq.(1a) then becomes

$$\mathbf{E_{scatt}}(r,0°;\rho_0,\varphi_0) = (\mathrm{i}E_0/kr)\exp(\mathrm{i}kr)\,\{[S_2(0°,\varphi;\rho_0,\varphi_0)\cos(\varphi) + S_1(0°,\varphi;\rho_0,\varphi_0)\sin(\varphi)]\,\mathbf{u_x}$$
$$+ [S_2(0°,\varphi;\rho_0,\varphi_0)\sin(\varphi) - S_1(0°,\varphi;\rho_0,\varphi_0)\cos(\varphi)]\,\mathbf{u_y}\}\ . \qquad (21)$$

Substituting Eqs.(19a),(19b) into Eq.(21), one obtains for an x-polarized incident beam

$$\mathbf{E_{scatt}}(r,0°;\rho_0,\varphi_0) = (\mathrm{i}E_0/kr)\exp(\mathrm{i}kr)\,\{\sum_{n=1}^{\infty} F_n\,(n+1/2)\,(a_n+b_n)\,\mathrm{I}_0(Q_n)\,\mathbf{u_x}$$

$$+ \sum_{n=1}^{\infty} F_n\,(n+1/2)\,(a_n-b_n)\,\mathrm{I}_2(Q_n)\,[\cos(2\varphi_0)\,\mathbf{u_x} + \sin(2\varphi_0)\,\mathbf{u_y}]\}\ . \qquad (22)$$

The terms in Eq.(22) proportional to $\mathbf{u_x}$ are the VV electric field, and the term proportional to $\mathbf{u_y}$ is the VH electric field.

For an incident y-polarized beam, substituting into Eqs.(17a),(17b) gives

$$S_1(0°,\varphi;\rho_0,\varphi_0) = -\sum_{n=1}^{\infty} F_n\,(n+1/2)\,(a_n+b_n)\,\mathrm{I}_0(Q_n)\cos(\varphi)$$

$$+ \sum_{n=1}^{\infty} F_n\,(n+1/2)\,(a_n-b_n)\,\mathrm{I}_2(Q_n)\cos(\varphi-2\varphi_0)\ , \qquad (23a)$$

$$S_2(0°,\varphi;\rho_0,\varphi_0) = \sum_{n=1}^{\infty} F_n\,(n+1/2)\,(a_n+b_n)\,\mathrm{I}_0(Q_n)\sin(\varphi)$$

$$- \sum_{n=1}^{\infty} F_n\,(n+1/2)\,(a_n-b_n)\,\mathrm{I}_2(Q_n)\sin(\varphi-2\varphi_0)\ . \qquad (23b)$$

The forward-scattered electric field is

$$\mathbf{E_{scatt}}(r,0°;\rho_0,\varphi_0) = (\mathrm{i}E_0/kr)\exp(\mathrm{i}kr)\,\{\sum_{n=1}^{\infty} F_n\,(n+1/2)\,(a_n+b_n)\,\mathrm{I}_0(Q_n)\,\mathbf{u_y}$$

$$+ \sum_{n=1}^{\infty} F_n\,(n+1/2)\,(a_n-b_n)\,\mathrm{I}_2(Q_n)\,[\sin(2\varphi_0)\,\mathbf{u_x} - \cos(2\varphi_0)\,\mathbf{u_y}]\}\ . \qquad (24)$$

The terms proportional to $\mathbf{u_y}$ in Eq.(24) are the HH electric field, and the term proportional to $\mathbf{u_x}$ is the HV electric field. It should be noted that for φ_0=-90°,180° for off-axis incidence either in the scattering plane or perpendicular to it, Eqs.(22),(24) give $\mathbf{E_{VH}}(0°)=\mathbf{E_{HV}}(0°)=0$.

Published in Journal of Quantitative Spectroscopy and Radiative Transfer 221 (2018) 260 - 272

The value of the GLMT angular functions in the back-scattering direction is

$$\tau_n^{\pm 1}(180°) = (-1)^n\, n(n+1)/2 \quad (25a)$$
$$\pi_n^{\pm 1}(180°) = -(-1)^n\, n(n+1)/2\ , \quad (25b)$$
$$\tau_n^{\pm m}(180°) = \pi_n^{\pm m}(180°) = 0 \text{ for } m \neq 1\ . \quad (25c)$$

For an x-polarized incident beam, substituting Eqs.(25a)-(25c) into Eqs.(14a),(14b) gives

$$S_1(180°,\varphi;\rho_0,\varphi_0) = -\sum_{n=1}^{\infty} F_n\,(n+1/2)\,(-1)^n\,(a_n-b_n)\,\mathrm{I}_0(Q_n)\,\sin(\varphi)$$
$$-\sum_{n=1}^{\infty} F_n\,(n+1/2)\,(-1)^n\,(a_n+b_n)\,\mathrm{I}_2(Q_n)\,\sin(\varphi-2\varphi_0)\ , \quad (26a)$$

$$S_2(180°,\varphi;\rho_0,\varphi_0) = \sum_{n=1}^{\infty} F_n\,(n+1/2)\,(-1)^n\,(a_{n\text{-}}b_n)\,\mathrm{I}_0(Q_n)\,\cos(\varphi)$$
$$+\sum_{n=1}^{\infty} F_n\,(n+1/2)\,(-1)^n\,(a_n+b_n)\,\mathrm{I}_2(Q_n)\,\cos(\varphi-2\varphi_0)\ . \quad (26b)$$

Evaluating $\mathbf{u_\theta}$ and $\mathbf{u_\varphi}$ at θ=180°, one obtains

$$\mathbf{u_\theta} = -\cos(\varphi)\,\mathbf{u_x} - \sin(\varphi)\,\mathbf{u_y} \quad (27a)$$

$$\mathbf{u_\varphi} = -\sin(\varphi)\,\mathbf{u_x} + \cos(\varphi)\,\mathbf{u_y}\ . \quad (27b)$$

The back-scattered electric field of Eq.(1a) then becomes

$$\mathbf{E_{scatt}}(r,180°;\rho_0,\varphi_0) = (\mathrm{i}E_0/kr)\exp(\mathrm{i}kr)\{[-S_2(180°,\varphi;\rho_0,\varphi_0)\cos(\varphi) + S_1(180°,\varphi;\rho_0,\varphi_0)\sin(\varphi)]\,\mathbf{u_x}$$
$$-[S_2(180°,\varphi;\rho_0,\varphi_0)\sin(\varphi) + S_1(180°,\varphi;\rho_0,\varphi_0)\cos(\varphi)]\,\mathbf{u}_\mathrm{y}\}\ . \quad (28)$$

Substituting Eqs.(26a),(26b) into Eq.(28), one obtains for an x-polarized incident beam

$$\mathbf{E_{scatt}}(r,180°;\rho_0,\varphi_0) = -(\mathrm{i}E_0/\mathrm{kr})\exp(\mathrm{i}kr)\{\sum_{n=1}^{\infty} F_n\,(n+1/2)\,(-1)^n\,(a_n-b_n)\,\mathrm{I}_0(Q_n)\,\mathbf{u_x}$$
$$-\sum_{n=1}^{\infty} F_n\,(n+1/2)\,(-1)^n\,(a_n+b_n)\,\mathrm{I}_2(Q_n)\,[\cos(2\varphi_0)\,\mathbf{u_x} + \sin(2\varphi_0)\,\mathbf{u_y}]\}\ . \quad (29)$$

The terms in Eq.(29) proportional to $\mathbf{u_x}$ are the VV electric field, and the term proportional to $\mathbf{u_y}$ is the VH electric field. For an incident y-polarized beam, substituting into Eqs.(17a),(17b) gives

$$S_1(180°,\varphi;\rho_0,\varphi_0) = \sum_{n=1}^{\infty} F_n\,(n+1/2)\,(-1)^n\,(a_n-b_n)\,\mathrm{I}_0(Q_n)\,\cos(\varphi)$$
$$+\sum_{n=1}^{\infty} F_n\,(n+1/2)\,(-1)^n\,(a_n+b_n)\,\mathrm{I}_2(Q_n)\,\cos(\varphi-2\varphi_0)\ , \quad (30a)$$

$$S_2(180°,\varphi;\rho_0,\varphi_0) = \sum_{n=1}^{\infty} F_n\,(n+1/2)\,(-1)^n\,(a_n-b_n)\,\mathrm{I}_0(Q_n)\,\sin(\varphi)$$
$$-\sum_{n=1}^{\infty} F_n\,(n+1/2)\,(-1)^n\,(a_n+b_n)\,\mathrm{I}_2(Q_n)\,\sin(\varphi-2\varphi_0)\ . \quad (30b)$$

Published in Journal of Quantitative Spectroscopy and Radiative Transfer 221 (2018) 260 - 272

The back-scattered electric field is

$$\mathbf{E}_{\mathbf{scatt}}(r,180°;\rho_0,\varphi_0) = -\,(\mathrm{i}E_0/kr)\exp(\mathrm{i}kr)\,\{\sum_{n=1}^{\infty} F_n\,(n+1/2)\,(-1)^n\,(a_n-b_n)\,\mathrm{I}_0(Q_n)\,\mathbf{u_y}$$

$$+\sum_{n=1}^{\infty} F_n\,(n+1/2)\,(-1)^n\,(a_n+b_n)\,\mathrm{I}_2(Q_n)\,[\cos(2\varphi_0)\,\mathbf{u_y} - \sin(2\varphi_0)\,\mathbf{u_x}]\} \quad . \qquad (31)$$

The terms proportional to $\mathbf{u_y}$ in Eq.(31) are the HH electric field, and the term proportional to $\mathbf{u_x}$ is the HV electric field. Again it should be noted that for φ_0=-90°,180°, Eqs.(29),(31) give $\mathbf{E_{VH}}$(180°)=$\mathbf{E_{HV}}$(180°)=0.

The form of the scattered electric field in the exact forward and backward directions in Eqs.(22),(24),(29),(31) due to an off-axis Gaussian beam has a formal structure that is identical to the structure of the scattered electric field in the near-forward and near-backward directions for an incident plane wave in Lorenz-Mie theory. In the near-forward direction where θ is small, let

$$\Theta_n \equiv (n+1/2)\,\theta \quad , \qquad (32)$$

and in the near-backward direction let

$$\Xi_n \equiv (n+1/2)\,(\pi-\theta) \quad . \qquad (33)$$

Then the near-forward scattered electric field for an incident x-polarized or y-polarized plane wave is found to be identical in structure to Eqs.(22),(24) with the substitutions $F_n\rightarrow1$, $\varphi_0\rightarrow\varphi$, $\mathrm{I}_0(Q_n)\rightarrow\mathrm{J}_0(\Theta_n)$, and $\mathrm{I}_2(Q_n)\rightarrow-\mathrm{J}_2(\Theta_n)$, where $\mathrm{J}_i(x)$ is a Bessel function. Similarly, the near-backward scattered electric field for an x-polarized or y-polarized plane wave is found to be identical in structure to Eqs.(29),(31) with the same substitutions, except that Ξ_n replaces Θ_n [35-37]. As to nomenclature, whereas in this study the term cross-polarized scattering is used to pertain to measurements made only in the scattering plane described in Sec.1, the same term is used in [37] to pertain to measurements made in all directions near back-scattering.

3. Numerical Example

Figures 2,3, respectively, show the exact VV and HH co-polarized GLMT scattered intensity for the following beam and particle and parameters. As in [13], the beam parameters are λ=0.5145µm for the green line of an argon ion laser, w_0=20µm, ρ_0=40µm, and the particle parameters are a=43.3µm, M=1.33. Whereas Eqs.(14)-(17) indicates that the sum over azimuthal modes m is performed first and the sum over partial waves n is performed last, the numerical evaluation of the double sum is more conveniently organized when the order of the sums is reversed [13]. In previous numerical studies, the maximum value of m computed, m_{max}, has often been taken to be m_{max}=10 for the beam and particle parameters considered here [38]. Additional numerical experimentation has now shown that although m_{max}=10 is sufficient for convergence for the co-polarized VV and HH scattering amplitudes, it is not sufficient for the much weaker cross-polarized VH and HV scattering amplitudes. Experimentation with m_{max}=20, 30, and 40 indicates that m_{max}=20 gives good convergence for the beam and particle parameters used here. The reason for this larger value for m_{max} for cross-polarized scattering will be discussed in [12]. For the remainder of this study and in [12], the sum over m is truncated at m_{max}=20 for all polarization channels.

The morphology of rainbows of various orders and the presence or absence of a Brewster angle intensity null are used here as diagnostics to assess whether the scattered intensity in any polarization channel is primarily TE- or TM-polarized. In Fig.2 the beam is translated off-axis in the φ=90° scattering plane with φ_0=-90°. The VV scattered intensity is TE-polarized. It is nearly identical to Fig.4a of [13] for 0°≤θ≤180°, and is nearly the mirror image of Fig.4c of [13] for 180°≤θ≤360°. The TE-polarized first- and second-order rainbows are clearly visible at θ≈138° and

Published in Journal of Quantitative Spectroscopy and Radiative Transfer 221 (2018) 260 - 272

$\theta \approx 233°$ respectively. The interference of the principal maximum of the third-order rainbow with external reflection is evident at $\theta \approx 315°$. Directly transmitted light dominates for $10° < \theta < 90°$, and the principal maximum of the TE-polarized fifth-order rainbow is present at $\theta \approx 130°$. The HH scattered intensity in Fig. 3 for $\varphi_0 = -90°$ is TM-polarized. The first- and second-order rainbows exhibit a number of supernumeraries without the presence of a strong principal maximum [39], and the Brewster angle for directly reflected light is evident at $\theta \approx 286°$. As mentioned at the end of Sec.2b, since the beam is translated off-axis in the scattering plane, the exact GLMT cross-polarized VH and HV scattered intensities vanish.

In Figs. 4,5, the beam is translated off-axis perpendicular to the $\varphi = 90°$ scattering plane with $\varphi_0 = 180°$ for the same beam and particle parameters as above. Whereas in Figs. 2,3 the scattering angle was plotted for $0° \leq \theta \leq 360°$, it is plotted in Figs. 4,5 for only $0° \leq \theta \leq 180°$ since the scattered intensity is exactly symmetric about $\theta = 180°$, as was mentioned at the end of Sec. 2b. The VV intensity qualitatively resembles the on-axis intensity of Fig.4b of [13]. The first- and second-order rainbows are absent in the rather featureless VV and HH intensities because the off-axis beam is only half as wide as the particle, and the beam center is incident on the particle far from the impact parameter of the first- and second-order rainbows, which is near the edge of the scattering plane. As was recently shown in [29] for scattering by an off-axis elliptical Gaussian beam, the cross-polarized VH and HV scattered intensities are nonzero. They are a number of orders of magnitude weaker than the co-polarized VV and HH intensities, and exhibit much interesting structure. The principal peak of the TE-polarized first-order rainbow at $\theta \approx 138°$ and a number of its supernumeraries are readily visible in the HV scattered intensity. Remnants of the TE-polarized second-order rainbow also appear at $\theta \approx 130°$. Some structure associated with the supernumeraries of the first-order TM rainbow, without the presence of a strong principal rainbow peak [39], are also evident in the VH scattered intensity at $\theta \approx 138°$. An explanation for this will be proposed in [12], based on the approximation to the scattering amplitudes developed there.

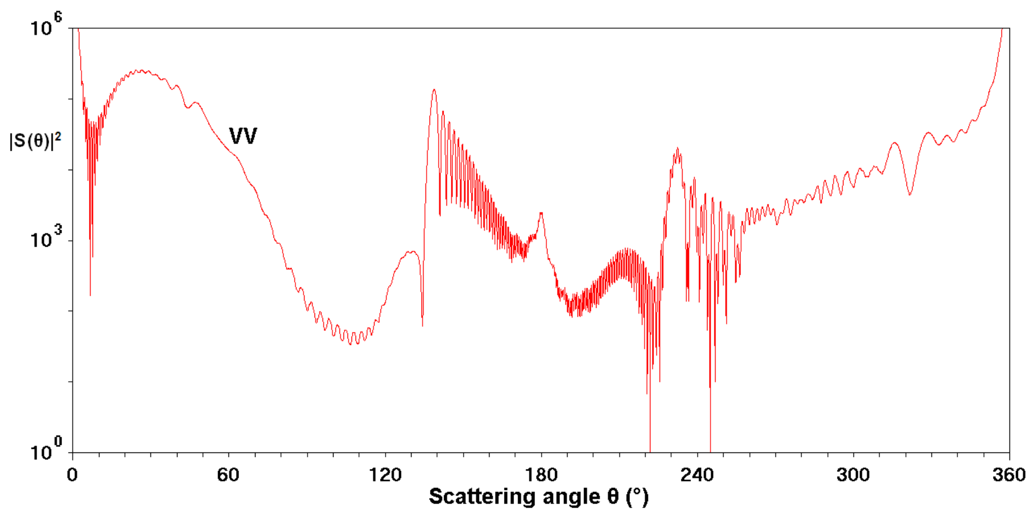

Fig. 2: Scattered intensity $|S_{VV}|^2$ as a function of the scattering angle θ for $0° \leq \theta \leq 360°$ for a Gaussian beam with $\lambda = 0.5145$µm, $w_0 = 20.0$µm incident on a homogeneous spherical particle with $a = 43.3$µm, $M = 1.33$. The scattering plane is $\varphi = 90°$, and the beam is off-axis in the scattering plane with $\rho_0 = 40$µm, $\varphi_0 = -90°$. The scattered intensity $|S_{VH}|^2$ is identically zero.

Published in Journal of Quantitative Spectroscopy and Radiative Transfer 221 (2018) 260 - 272

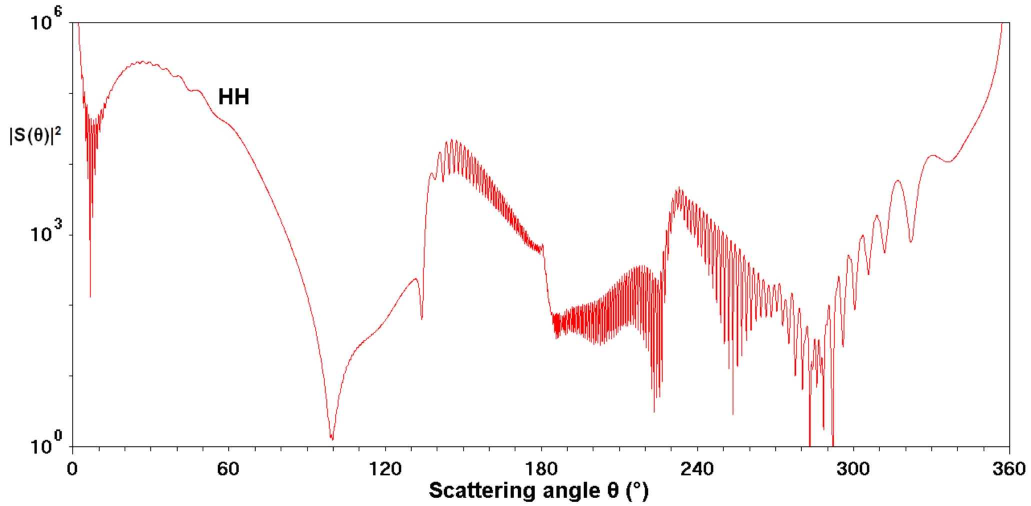

Fig. 3: Scattered intensity $|S_{HH}|^2$ as a function of the scattering angle θ for the same beam, particle, and detector plane parameters as in Fig. 2. $|S_{HV}|^2$ is identically zero.

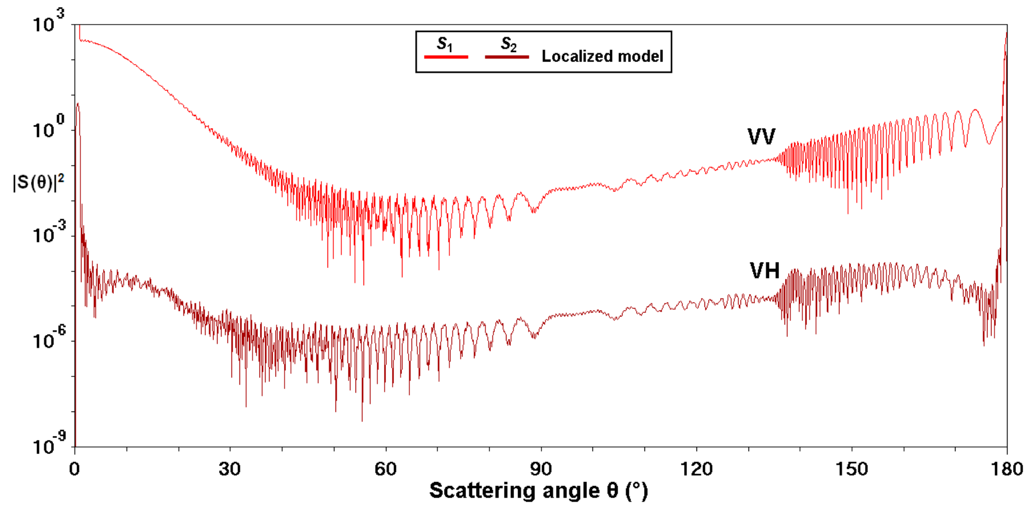

Fig. 4: Scattered intensity $|S_{VV}|^2$ and $|S_{VH}|^2$ as a function of the scattering angle θ for $0° \leq \theta \leq 180°$ for the Gaussian beam and particle of Fig.2. The scattering plane is φ=90°, and the beam is off-axis perpendicular to the scattering plane with ρ_0=40µm, φ_0=180°.

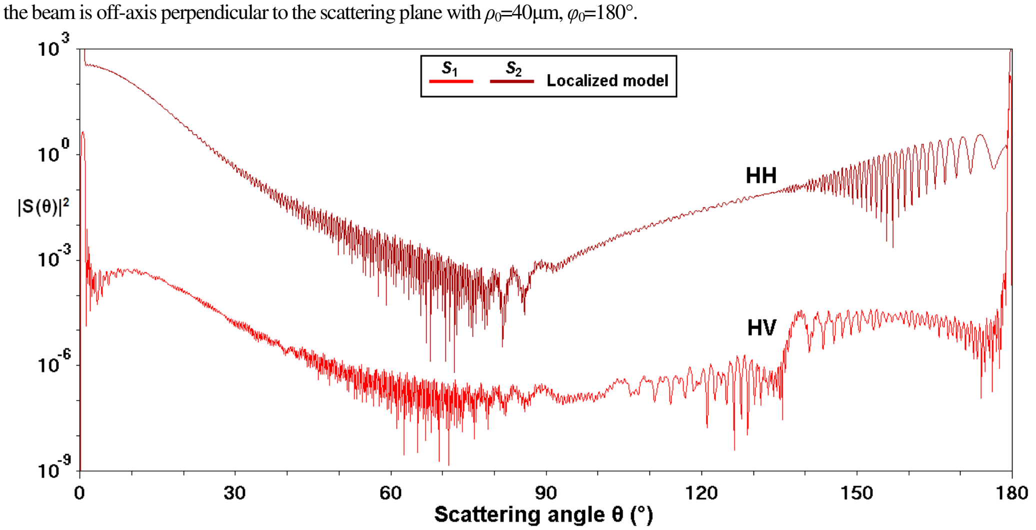

Fig. 5: Scattered intensity $|S_{HH}|^2$ and $|S_{HV}|^2$ as a function of the scattering angle θ for the same beam, particle, and detector plane parameters as in Fig. 2.

Published in Journal of Quantitative Spectroscopy and Radiative Transfer 221 (2018) 260 - 272

4. Symmetry Breaking and Cross-Polarized Scattering

4a. Ray Theory for Plane Wave Incidence

In Subsections 4a-4c, ray theory ideas are used to motivate various approximations to the wave theory scattering amplitudes that will be found to be useful in the second part of this study [12]. As a first example, let an x-polarized plane wave with electric field strength E_0 be incident on a spherical particle. The scattering amplitudes of Eqs.(1a),(1b) are separable in θ and φ with

$$S_1(\theta,\varphi) = S_1(\theta)\sin(\varphi) \tag{34a}$$

$$S_2(\theta,\varphi) = S_2(\theta)\cos(\varphi)\ , \tag{34b}$$

where $S_1(\theta)$ and $S_2(\theta)$ are the Lorenz-Mie scattering amplitudes (see p.125 of [7] and Eq.(4.74) of [8]),

$$S_1(\theta) = \sum_{n=1}^{\infty} c_n\,[a_n\,\pi_n^{\,1}(\theta) + b_n\,\tau_n^{\,1}(\theta)] \tag{35a}$$

$$S_2(\theta) = \sum_{n=1}^{\infty} c_n\,[a_n\,\tau_n^{\,1}(\theta) + b_n\,\pi_n^{\,1}(\theta)]\ . \tag{35b}$$

Similarly, the scattering amplitudes for a y-polarized incident plane wave are

$$S_1(\theta,\varphi) = -\,S_1(\theta)\cos(\varphi) \tag{36a}$$

$$S_2(\theta,\varphi) = S_2(\theta)\sin(\varphi)\ . \tag{36b}$$

An incident plane wave can be modeled by a large group of parallel geometrical rays, each of magnitude E_0 and propagating in the $+z$ direction. Rays incident in the scattering plane at the sphere's equator will remain in the same plane after scattering. If the scattering plane is the horizontal yz plane, substitution of φ=±90° into Eqs.(34),(36) gives

$$S_{VV}(\theta,\varphi=\pm 90°) = \pm S_1(\theta) \tag{37a}$$

$$S_{HH}(\theta,\varphi=\pm 90°) = \pm S_2(\theta) \tag{37b}$$

$$S_{VH}(\theta,\varphi=\pm 90°) = S_{HV}(\theta,\varphi=90°) = 0\ . \tag{37c}$$

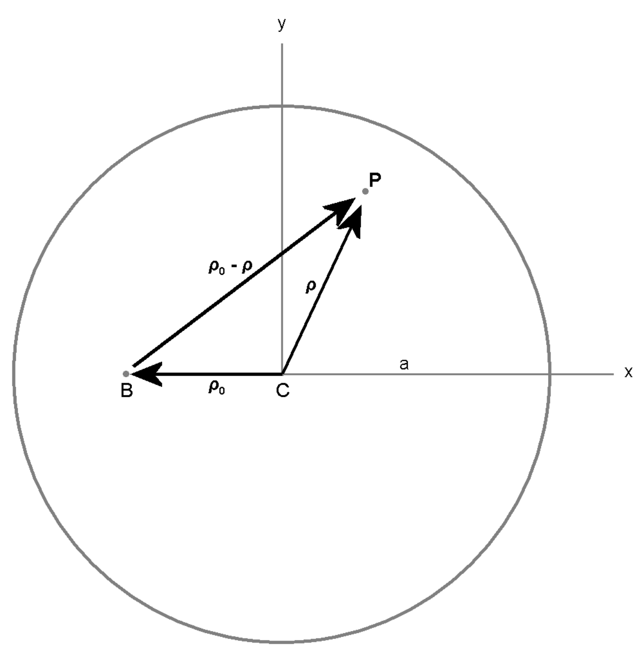

Fig. 6: Geometry of a Gaussian beam incident off-axis with respect to a spherical particle of radius a. The center of the particle is C, the beam axis is B, and P is an arbitrary point in the z=0 plane.

Published in Journal of Quantitative Spectroscopy and Radiative Transfer 221 (2018) 260 - 272

4b. Ray Theory for On-Axis Gaussian Beam Incidence

The Gaussian beam considered in Sec. 3 has λ=0.5145μm and w_0=20μm, and the scattering particle has a=43.3μm. The beam confinement parameter of Eq.(7) is s=4.09×10^{-3}, and the half-length of the beam focal waist is

$$L/2 = kw_0^2/2 = 2443\ \mu\text{m}\ . \qquad (38)$$

Since $w_0 \gg \lambda$ and $(L/2) \gg a$, the beam barely changes its shape in the vicinity of the scattering particle at the center of its focal waist. Thus it is not unreasonable to extend ray theory ideas to this situation. The simplest approximate model of an x-polarized Gaussian beam is an infinitely long tube of electric and magnetic field of unchanging half-width w_0. As was mentioned in Sec. 2 and is illustrated in Fig.6, the center of the scattering particle and the center of the beam's focal waist both lie in the same plane transverse to the beam axis. The center of the particle coincides with the origin of the coordinate system, and the vector from this origin to an arbitrary point in the transverse plane is $\boldsymbol{\rho}$. The vector from the origin to the beam axis is $\boldsymbol{\rho}_0$, and the vector from the beam axis to the same arbitrary point in the transverse plane is $\boldsymbol{\rho}$-$\boldsymbol{\rho}_0$. If the Gaussian beam is on-axis with respect to the scattering particle, this simple model of the electric field gives

$$\begin{aligned}\mathbf{E}^{\text{on-axis}} &\approx E_0 \exp(ikz) \exp[-|\boldsymbol{\rho}|^2/w_0^2]\ \mathbf{u_x} \\ &= E_0 \exp(ikz) \exp[-s^2(k\rho)^2]\ \mathbf{u_x}\ , \qquad (39)\end{aligned}$$

which is independent of the azimuthal angle φ. This was also the case for an incident plane wave.

The localization principle of van de Hulst (see pp.208-209 of [7]) can be used to associate the ray impact parameter $k\rho$ with the partial wave $(n+1/2)$ to give the magnitude, A_n, of an effective ray of the Gaussian beam. This ray magnitude is then substituted into Eqs.(35a),(35b) of Lorenz-Mie theory to give our ray-theory-based approximation to the co-polarized GLMT scattering amplitudes for an incident Gaussian beam,

$$S_{VV}(\theta) \approx \sum_{n=1}^{\infty} c_n A_n \left[a_n \pi_n^1(\theta) + b_n \tau_n^1(\theta)\right] \qquad (40a)$$

$$S_{HH}(\theta) \approx \sum_{n=1}^{\infty} c_n A_n \left[a_n \tau_n^1(\theta) + b_n \pi_n^1(\theta)\right]\ . \qquad (40b)$$

Since the effective rays of the Gaussian beam are incident in the horizontal scattering plane at the sphere's equator, they remain in the horizontal plane after scattering with the same polarization as the incident rays. Thus ray theory for Gaussian beam scattering again predicts that

$$S_{VH}(\theta) = S_{HV}(\theta) = 0\ . \qquad (41)$$

For the on-axis Gaussian beam of Eq.(39), one has

$$A_n = \exp[-s^2(n+1/2)^2] \qquad (42)$$

as the magnitude of an effective ray. Equations (40a),(40b) for the VV and HH scattering amplitudes with the on-axis effective ray magnitude of Eq.(42) are identical to the VV and HH scattering amplitudes that have been obtained for the localized model of an on-axis Gaussian beam, and that have been rigorously derived using the generalized Lorenz-Mie theory of wave scattering without appealing to ray theory ideas [24].

For $0° \ll \theta \ll 180°$ and $(n+1/2) \gg 1$, the amplitude of the oscillatory function $\tau_n^1(\theta)$ is much larger than that of $\pi_n^1(\theta)$, and Eqs.(40a),(40b) can be further approximated as

$$S_{VV}(\theta) \approx \sum_{n=1}^{\infty} c_n b_n A_n \tau_n^1(\theta) \qquad (43a)$$

$$S_{HH}(\theta) \approx \sum_{n=1}^{\infty} c_n a_n A_n \tau_n^1(\theta)\ . \qquad (43b)$$

Published in Journal of Quantitative Spectroscopy and Radiative Transfer 221 (2018) 260 - 272

Equations (43a),(43b) will be found in Sec. 4 of [12] to be identical to an approximation to the co-polarized scattering amplitudes for both on-axis and off-axis beam incidence, derived there using the generalized Lorenz-Mie theory of wave scattering. We will show there that for off-axis beam incidence, an approximation to the GLMT angular functions permits the sum over azimuthal modes *m* to be evaluated analytically, leaving only a sum over partial waves *n*, of the form of Eqs.(43a),(43b).

4c. Ray Theory for Off-Axis Gaussian Beam Incidence

We now assume that the Gaussian beam is off-axis with respect to the scattering particle, giving

$$\mathbf{E}^{\textbf{off-axis}} \approx E_0 \exp(ikz) \exp[-|\boldsymbol{\rho}\text{-}\boldsymbol{\rho}_0|^2/w_0^2]\ \mathbf{u_x}$$
$$= E_0 \exp(ikz) \exp[-s^2(k\rho)^2] \exp(-\rho_0^2/w_0^2) \exp[\varepsilon\ (k\rho) \cos(\varphi\text{-}\varphi_0)]\ \mathbf{u_x} \quad , \qquad (44)$$

where

$$\varepsilon \equiv 2s\rho_0/w_0 \quad . \qquad (45)$$

Equation (44) explicitly depends on φ and is no longer circularly symmetric with respect to the coordinate system whose origin coincides with the center of the particle. Using the same ray-theory-based approximation for this off-axis Gaussian beam, along with the van de Hulst localization principle, the magnitude of an effective ray in Eq.(44) is

$$A_n = F_n \exp[(n+1/2)\,\varepsilon \cos(\varphi\text{-}\varphi_0)] \quad , \qquad (46)$$

where F_n was defined in Eq.(10). If the beam is off-axis in the horizontal scattering plane with φ=90°, φ_0=-90°, then the effective ray magnitude of Eq.(46) reduces to

$$A_n = F_n \exp[(n+1/2)\ \varepsilon] \quad . \qquad (47)$$

This is then substituted into Eqs.(40a),(40b) or Eqs.(43a),(43b) to give a ray-theory-based approximation to the VV and HH scattering amplitudes. If the beam is off-axis perpendicular to the scattering plane with φ=90°, φ_0=180°, then the effective ray magnitude is

$$A_n = F_n \quad . \qquad (48)$$

This is again substituted into Eqs.(40),(43) to give the ray-theory-based co-polarized scattering amplitudes.

The ray-theory-based absence of cross-polarized scattering in Eq.(41) conflicts with the nonzero VH and HV scattering found in Figs.4,5. Thus cross-polarized scattering will have to be understood in the context of wave theory. This claim will be reinforced in the next subsection where the magnitude of $S_{VH}(\theta)$ and $S_{HV}(\theta)$ is found to be of order $\varepsilon=\lambda\rho_0/\pi w_0^2$, when compared to the magnitude of the dominant scattering amplitudes $S_{VV}(\theta)$ and $S_{HH}(\theta)$. This scaling factor is wavelength dependent, indicating that it is a wave theory effect. If nonzero cross-polarized scattering were to be explainable as purely a ray theory effect, the overall magnitude of $S_{VH}(\theta)$ and $S_{HV}(\theta)$ would have to be independent of λ. This is because in the short-wavelength limit, the portion of $S_{VV}(\theta)$ and $S_{HH}(\theta)$ corresponding to geometrical optics (see Sec. 5 of [40]) scales as (ka), and when combined with the 1/(kr) factor in Eqs.(1a),(1b), gives scattered VV and HH fields that are independent of λ.

4d. Symmetry Breaking in Wave Theory

The fact that nonzero cross-polarized scattering is a consequence of wave theory symmetry breaking may be motivated in two stages. The first stage relies on the mathematics of the coupling of angular momentum states which is familiar in quantum mechanical scattering, (see Sec.16.2 of [41]). The on-axis *x*-polarized Gaussian beam of Eq.(39) can be written as

$$\mathbf{E}^{\textbf{on-axis}} \approx E_0 \exp(ikz) \exp[-|\boldsymbol{\rho}|^2/w_0^2]\ \mathbf{u_x}$$
$$= E_0 \sum_{n=0}^{\infty} \mathrm{i}^n\ (2n+1)\ \mathrm{j}_n(kr)\ \mathrm{P}_n^{\,0}[\cos(\theta)] \exp[-r^2\sin^2(\theta)/w_0^2]\ (-\,\mathbf{u}_+ + \mathbf{u}_-)/2^{1/2} \quad , \qquad (49)$$

Published in Journal of Quantitative Spectroscopy and Radiative Transfer 221 (2018) 260 - 272

(see Eq.(11.56) of [41]), where $j_n(kr)$ is a spherical Bessel function and $\mathbf{u}_+$ and $\mathbf{u}_-$ are the circular polarization states (see Eq.(16.111) of [41])

$$\mathbf{u}_+ = -(\mathbf{u_x} + i\,\mathbf{u_y})/2^{1/2} \quad (50a)$$

$$\mathbf{u}_- = (\mathbf{u_x} - i\,\mathbf{u_y})/2^{1/2} \ . \quad (50b)$$

Since the beam in Eq.(49) is independent of the azimuthal angle φ, the Legendre function $P_n^0[\cos(\theta)]$ is a state of orbital angular momentum whose magnitude is n and whose z-component is n_z=0. Similarly, the circular polarization unit vectors $\mathbf{u}_+$ and $\mathbf{u}_-$ are states of angular momentum whose magnitude is s=1 and whose z-component is m_s=±1. Equation (49) thus contains the product of two angular momentum states, and as such, it is called an uncoupled representation of the electric field. According to the mathematics of group theory, a product representation of the rotation group may be expressed as a direct sum of a number of irreducible representations (see Eq.(16.87) of [41]). Thus in the coupled representation of a linearly polarized on-axis beam, the two separate angular momenta are combined into total angular momentum states (see Sec.16.6 of [41]) whose magnitude j is constrained to integer steps in the interval

$$|n - s| \leq j \leq n + s \quad (51a)$$

and whose z-component is

$$m_j = m_n + m_s \ . \quad (51b)$$

For the example of an on-axis beam of Eq.(49), the coupled angular momentum states have partial wave numbers n+1, n, and n-1, and z-component m_j=±1. The j=n+1 and j=n-1 states taken together can be shown to be electric multipole or TM waves, while the j=n states can be shown to be magnetic multipole or TE waves, each of which are described in terms of the Lorenz-Mie angular functions (see Sec.9.31 of [7]) $\tau_n^{\pm 1}(\theta)$ and $\pi_n^{\pm 1}(\theta)$.

In like manner, the x-polarized off-axis Gaussian beam of Eq.(43) can be written as

$$\mathbf{E}^{\text{off-axis}} \approx E_0 \exp(ikz) \exp[-|\boldsymbol{\rho}-\boldsymbol{\rho}_0|^2/w_0^2]\, \mathbf{u_x}$$

$$= E_0 \sum_{n=0}^{\infty} i^n (2n+1)\, j_n(kr)\, P_n^0[\cos(\theta)] \exp[-r^2\sin^2(\theta)/w_0^2]$$

$$\times \exp(-\rho_0^2/w_0^2) \exp[\varepsilon\,(k\rho)\cos(\varphi-\varphi_0)]\, (-\mathbf{u}_+ + \mathbf{u}_-)/2^{1/2} \ . \quad (52)$$

The beam of Eq.(52) now explicitly depends on the azimuthal angle φ. Because of this, if the φ-dependent exponential were expanded in terms of a sum of spherical harmonics, (i.e. angular momentum states), with partial wave number $n_{off\text{-}axis}$ and azimuthal mode number $m_{off\text{-}axis}$, the sum would contain all values of $m_{off\text{-}axis}$. When these off-axis angular momentum states are coupled to both the orbital angular momentum states of $P_n^0[\cos(\theta)]$ and the angular momentum states of the circular polarization unit vectors $\mathbf{u}_+$ and $\mathbf{u}_-$, they give rise to the GLMT scattering amplitudes S_1 and S_2 containing sums over all azimuthal modes m as in Eqs.(14),(17) which are described by the full range of GLMT angular functions $\tau_n^m(\theta)$ and $\pi_n^m(\theta)$.

In order to more clearly understand why there is a larger range of m values for an off-axis beam than there was for an on-axis beam, let the beam be translated only slightly off-axis with $0<\varepsilon \ll 1/k\rho$. One can then Taylor series expand the $\exp[\varepsilon\,(k\rho)\cos(\varphi-\varphi_0)]$ factor in Eq.(52) to obtain

$$\exp[\varepsilon\,(k\rho)\cos(\varphi-\varphi_0)] \approx 1 + \varepsilon\,(k\rho)\cos(\varphi-\varphi_0) + O(\varepsilon^2) \quad (53)$$

The first term of Eq.(53) is independent of φ, and thus is circularly symmetric, corresponding to $m_{off\text{-}axis}$=0 and m_j=±1, as was the case for an on-axis beam and a plane wave. The second term varies sinusoidally in φ, corresponding to $m_{off\text{-}axis}$=±1, and is not circularly symmetric . Coupling these states to both the m_n=0 states of the Legendre polynomials and the m_s=±1 states of the circular polarization unit vectors, one obtains the spherical multipole radiation states with the larger range of azimuthal modes, m_j=0, ±1, ±2. Progressively higher order terms in the Taylor series expansion produce an increasingly wider range of m_j values.

The second stage of the wave theory analysis uses this fact along with the properties of the beam shape coefficients to show that cross-polarized scattering is identically zero for an on-axis beam, and that this results from

Published in Journal of Quantitative Spectroscopy and Radiative Transfer 221 (2018) 260 - 272

the spherical symmetry of the beam with respect to the coordinate system with its origin at the center of the particle. Consider the case when the Gaussian beam first begins to be translated off-axis. Omitting constants of proportionality, Eqs.(4a),(4b) for the beam shape coefficients may be rewritten as

$$A_{nm}^{+} \sim \int_0^{2\pi} \mathrm{d}\varphi \cos(m\varphi)\, E_{inc}^{rad}(r,\theta,\varphi) \qquad (54a)$$

$$A_{nm}^{-} \sim -\,\mathrm{i} \int_0^{2\pi} \mathrm{d}\varphi \sin(m\varphi)\, E_{inc}^{rad}(r,\theta,\varphi) \qquad (54b)$$

$$B_{nm}^{+} \sim \int_0^{2\pi} \mathrm{d}\varphi \cos(m\varphi)\, cB_{inc}^{rad}(r,\theta,\varphi) \qquad (54c)$$

$$B_{nm}^{-} \sim -\,\mathrm{i} \int_0^{2\pi} \mathrm{d}\varphi \sin(m\varphi)\, cB_{inc}^{rad}(r,\theta,\varphi)\ , \qquad (54d)$$

where the integral over θ and all the other multiplicative factors have been left implicit. For the simple model of the x-polarized on-axis beam considered in Eq.(49), the radial component of the electric field is proportional to $\sin(\theta)\cos(\varphi)$ and the radial component of the magnetic field is proportional to $\sin(\theta)\sin(\varphi)$. Then Eqs.(54a)-(54d) give

$$A_{n1}^{+} \sim \mathrm{i}\, B_{n1}^{-} \sim \pi \qquad (55a)$$

$$A_{n1}^{-} = B_{n1}^{+} = 0 \qquad (55b)$$

$$A_{nm}^{\pm} = B_{nm}^{\pm} = 0 \text{ for } m\neq 1, \qquad (55c)$$

in agreement with addition of angular momentum results mentioned above, and again with all the identical θ dependence left implicit. For the simple model of the corresponding y-polarized on-axis beam whose radial component of the electric field is proportional to $\sin(\theta)\sin(\varphi)$ and whose radial component of the magnetic field is proportional to $-\sin(\theta)\cos(\varphi)$, Eqs.(54a)-(54d) give

$$A_{n1}^{+} = B_{n1}^{-} = 0 \qquad (56a)$$

$$B_{n1}^{+} \sim -\mathrm{i}\, A_{n1}^{-} \sim -\pi \qquad (56b)$$

$$A_{nm}^{\pm} = B_{nm}^{\pm} = 0 \text{ for } m\neq 1\ . \qquad (56c)$$

According to Eqs.(2a),(2b) in the φ=90° scattering plane, the m=±1 portion of the scattering amplitudes is

$$S_1(\theta,90°) = \sum_{n=1}^{\infty} c_n\, [\mathrm{i}\, B_{n1}^{-}\, b_n\, \tau_n^{1}(\theta) + A_{n1}^{+}\, a_n\, \pi_n^{1}(\theta)] \qquad (57a)$$

$$S_2(\theta,90°) = \sum_{n=1}^{\infty} c_n\, [\mathrm{i}\, A_{n1}^{-}\, a_n\, \tau_n^{1}(\theta) - B_{n1}^{+}\, b_n\, \pi_n^{1}(\theta)]\ . \qquad (57b)$$

Substitution of Eq.(55b) for an x-polarized beam into Eq.(57b) gives $S_{VH}(\theta,90°)=0$, and substitution of Eq.(56a)for a y-polarized beam into Eq.(57a) gives $S_{HV}(\theta,90°)=0$. Thus if the beam is on-axis, crossed-polarized scattering cannot occur.

Consider now an x-polarized off-axis Gaussian beam and keep the non-circularly symmetric term in Eq.(53) that is first order in ε. Using van de Hulst's localization principle to associate the impact parameter $k\rho$ with the partial wave number n+1/2, Eqs.(54a)-(54d) for the beam shape coefficients for m=0 are

$$A_n^{0} \sim (n+1/2)\, \varepsilon\pi \cos(\varphi_0) \qquad (58a)$$

$$B_n^{0} \sim (n+1/2)\, \varepsilon\pi \sin(\varphi_0)\ , \qquad (58b)$$

and for m = ±2 they are

$$A_{n2}^{+} \sim \mathrm{i}\, B_{n2}^{-} \sim (n+1/2)\, (\varepsilon\pi/2) \cos(\varphi_0) \qquad (58c)$$

$$B_{n2}^{+} \sim -\mathrm{i}\, A_{n2}^{-} \sim (n+1/2)\, (-\varepsilon\pi/2) \sin(\varphi_0). \qquad (58d)$$

Published in Journal of Quantitative Spectroscopy and Radiative Transfer 221 (2018) 260 - 272

The beam shape coefficients are zero for $m \neq 0,2$, in agreement with the addition of angular momentum results mentioned above. For an off-axis y-polarized beam, again to first order in ε, the beam shape coefficients for $m = 0$ are

$$A_n^0 \sim (n+1/2)\,\varepsilon\pi\,\sin(\varphi_0) \qquad (59a)$$

$$B_n^0 \sim (n+1/2)\,\varepsilon\pi\,\cos(\varphi_0) \qquad (59b)$$

and for $m=\pm 2$ they are

$$A_{n2}^{+} \sim \mathrm{i}\,B_{n2}^{-} \sim (n+1/2)\,(-\varepsilon\pi/2)\,\sin(\varphi_0) \qquad (59c)$$

$$B_{n2}^{+} \sim -\mathrm{i}\,A_{n2}^{-} \sim (n+1/2)\,(-\varepsilon\pi/2)\,\cos(\varphi_0). \qquad (59d)$$

The beam shape coefficients are again zero for $m \neq 0,2$.

According to Eqs.(2a),(2b) in the $\varphi=90°$ scattering plane, the $m=0$ portion of the scattering amplitudes is

$$S_1(\theta,90°) = (1/2)\sum_{n=1}^{\infty} c_n\,B_n^0\,b_n\,\tau_n^0(\theta) \qquad (60a)$$

$$S_2(\theta,90°) = (1/2)\sum_{n=1}^{\infty} c_n\,A_n^0\,a_n\,\tau_n^0(\theta)\ , \qquad (60b)$$

and the $m=\pm 2$ portion is

$$S_1(\theta,90°) = \sum_{n=1}^{\infty} c_n\,[-B_{n2}^{+}\,b_n\,\tau_n^2(\theta) + \mathrm{i}\,A_{n2}^{-}\,a_n\,2\pi_n^2(\theta)] \qquad (61a)$$

$$S_2(\theta,90°) = \sum_{n=1}^{\infty} c_n\,[-A_{n2}^{+}\,a_n\,\tau_n^2(\theta) - \mathrm{i}\,B_{n2}^{-}\,b_n\,2\pi_n^2(\theta)]\ . \qquad (61b)$$

Substitution of Eqs.(58a),(58c) for an x-polarized beam into Eqs.(60b),(61b) for the VH scattering amplitude gives a nonzero result proportional to $(n+1/2)\,\varepsilon\cos(\varphi_0)$. Similarly, substitution of Eqs.(59b),(59d) for a y-polarized beam into Eqs.(60a),(61a) for the HV scattering amplitude gives a nonzero result also proportional to $(n+1/2)\,\varepsilon\cos(\varphi_0)$. This is consistent with the observation at the end of Sec.2 that cross-polarized scattering cannot occur when the beam is translated off-axis in the scattering plane. In like manner, substitution of Eqs.(58b),(58d) for an x-polarized beam into Eqs.(60a),(61a) gives a correction to the VV scattering amplitude for off-axis incidence in the scattering plane, and substitution of Eqs.(59a),(59c) for a y-polarized beam into Eqs.(60b),(61b) gives a correction to the HH scattering amplitude for off-axis incidence in the scattering plane. The $m=0,\pm 2$ azimuthal modes of S_1 and S_2 are the first to join the circular symmetric $m=\pm 1$ Lorenz-Mie modes to produce the onset of VH and HV cross-polarized scattering as the beam begins to be translated off-axis out of the scattering plane. The amplitude of cross-polarized scattering is found in [12] to continue to be proportional to ε as the beam is translated off-axis by larger distances.

4e. Cross-Polarized Scattering and Davis Beams

A focused Gaussian beam can be nearly equally well described in terms of either the localized beam model or the Davis beam model [42,43], as long as $w_0 \gg \lambda$. The localized beam is defined by the value of the beam shape coefficients A_n^m and B_n^m, and the field components are then derived from them. Complementary to this, Davis beams are defined in terms of a series expansion in powers of s of the field components, and the beam shape coefficients can then be obtained from them. The series expansion of the rectangular components of the Davis model of an x-polarized Gaussian beam results from the constraint that the fields must satisfy Maxwell's equations. The lowest order contribution to the x-component of the electric field is of order s^0, and the lowest order contribution to the z-component and the y-component is of order s^1 and s^2, respectively. The structure of the components of the Davis

Published in Journal of Quantitative Spectroscopy and Radiative Transfer 221 (2018) 260 - 272

magnetic field is similar. Although the electric and magnetic fields of such a beam are in the x and y directions at the center of the beam waist, respectively, the electric field acquires small z and y components and the magnetic field acquires small z and x components elsewhere. The details of the Davis model of a y-polarized Gaussian beam are similar.

Consider an x-polarized Davis beam centered on the off-axis position (x_0, y_0, z_0=0). The beam fields, to lowest order in s for each of the rectangular components are [42,43]

$$\mathbf{E}^{\mathbf{Davis}}(x,y,z) = E_0 D \exp(\mathrm{i}kz) \exp[-D(x-x_0)^2/w_0^2] \exp[-D(y-y_0)^2/w_0^2] \times \{\mathbf{u_x} + [2s^2D^2(x-x_0)(y-y_0)/w_0^2]\, \mathbf{u_y} - [2\mathrm{i}sD(x-x_0)/w_0]\, \mathbf{u_z}\} \tag{62a}$$

$$\mathbf{B}^{\mathbf{Davis}}(x,y,z) = (E_0 D/c) \exp(\mathrm{i}kz) \exp[-D(x-x_0)^2/w_0^2] \exp[-D(y-y_0)^2/w_0^2] \times \{[2s^2D^2(x-x_0)(y-y_0)/w_0^2]\, \mathbf{u_x} + \mathbf{u_y} - [2\mathrm{i}sD(y-y_0)/w_0]\, \mathbf{u_z}\} \quad , \tag{62b}$$

where the diffractive spreading of the beam as a function of z is given by

$$D = [1 + 2\mathrm{i}sz/w_0]^{-1} \quad . \tag{63}$$

Expressing the rectangular coordinates (x,y) and (x_0,y_0) in terms of polar coordinates (ρ,φ) and (ρ_0,φ_0) as in Fig.6, using ε of Eq.(45) as a measure of the off-axis distance, and neglecting the diffractive spreading D of Eq.(63), Eqs.(62a),(62b) become

$$\mathbf{E}^{\mathbf{Davis}}(\rho,\varphi,z;\rho_0,\varphi_0) = E_0 \exp(\mathrm{i}kz) \exp[-s^2(k\rho)^2] \exp(-\rho_0^2/w_0^2) \exp[\varepsilon\,(k\rho)\cos(\varphi-\varphi_0)] \times \{\mathbf{u_x} + [s^4 (k\rho)^2 \sin(2\varphi) - s^2\varepsilon\,(k\rho)\sin(\varphi+\varphi_0) + (\varepsilon^2/4)\sin(2\varphi_0)]\, \mathbf{u_y} + [-2\mathrm{i}s^2 (k\rho)\cos(\varphi) + \mathrm{i}\varepsilon\cos(\varphi_0)]\, \mathbf{u_z}\} \tag{64a}$$

$$\mathbf{B}^{\mathbf{Davis}}(\rho,\varphi,z;\rho_0,\varphi_0) = (E_0/c) \exp(\mathrm{i}kz) \exp[-s^2(k\rho)^2] \exp(-\rho_0^2/w_0^2) \exp[\varepsilon\,(k\rho)\cos(\varphi-\varphi_0)] \times \{[s^4 (k\rho)^2 \sin(2\varphi) - s^2\varepsilon\,(k\rho)\sin(\varphi+\varphi_0) + (\varepsilon^2/4)\sin(2\varphi_0)]\, \mathbf{u_x} + \mathbf{u_y} + [-2\mathrm{i}s^2 (k\rho)\sin(\varphi) + \mathrm{i}\varepsilon\sin(\varphi_0)]\, \mathbf{u_z}\} \tag{64b}$$

If one were to apply ray theory ideas to this beam, one would first evaluate the beam at the intersection of the φ=±90° scattering plane with the sphere equator. The electric field of an x-polarized beam at the particle surface is

$$\mathbf{E}^{\mathbf{Davis}} = E_0 \exp[-\mathrm{i}ka\cos(\theta_i)] \exp[-s^2(k\rho)^2] \exp(-\rho_0^2/w_0^2) \exp[\varepsilon\,(k\rho)\sin(\varphi_0)] \times [\mathbf{u_x} \mp s^2\varepsilon\,(k\rho)\cos(\varphi_0)\, \mathbf{u_y} + (\varepsilon^2/4)\sin(2\varphi_0)\, \mathbf{u_y} + \mathrm{i}\varepsilon\cos(\varphi_0)\, \mathbf{u_z}] \quad , \tag{65}$$

where θ_i is the angle of incidence of an effective ray at the surface of the sphere. The expression for $\mathbf{B}^{\mathbf{Davis}}$ at the sphere surface is similar. For in-plane off-axis incidence with φ_0=90° and using the van de Hulst localization principle, the effective ray magnitude vector of Eq.(65) is

$$\mathbf{A_n} = F_n \exp[\varepsilon\,(n+1/2)]\, \mathbf{u_x} \tag{66}$$

as in Eq.(47). For off-axis incidence perpendicular to the scattering plane with φ_0=180°, the effective ray magnitude vector is

$$\mathbf{A_n} = F_n [\mathbf{u_x} + s^2\varepsilon\,(n+1/2)\, \mathbf{u_y} - \mathrm{i}\varepsilon\, \mathbf{u_z}] \ , \tag{67}$$

which provides small $\mathbf{u_y}$ and $\mathbf{u_z}$ correction terms to Eq.(48). For an incident x-polarized Gaussian beam (i.e. incident V as in Sec.1) and off-axis incidence perpendicular to the scattering plane, there is a small induced y-polarized field of strength $s^2\varepsilon$ (n+1/2) relative to that of the dominant x-polarized electric field. If one were to now apply the previously used ray-theory-based ideas to this y-polarized correction field, since it is incident in the horizontal scattering plane it will also exit the sphere in the scattering plane (i.e. outgoing H as in Sec.1). One might be tempted to conjecture that it can be identified as the physical mechanism producing the cross-polarized VH scattering observed in Fig.4. But

Published in Journal of Quantitative Spectroscopy and Radiative Transfer 221 (2018) 260 - 272

this cannot be the case since both in Sec.4c and in [12] it is seen that the dominant term in the VH scattering amplitude is of order ε relative to the dominant VV scattering amplitude. The Davis beam y-polarized correction field discussed here is instead an order s^2 correction to the dominant term.

Now consider the z component of $\mathbf{E}^{\mathbf{Davis}}$ and $\mathbf{B}^{\mathbf{Davis}}$ in the context of wave theory. Let the electric field of the incident beam be nominally x-polarized and propagate in the z direction. The Maxwell equation

$$\nabla \bullet \mathbf{E} = 0 \qquad (68a)$$

can be loosely written for this situation as

$$\partial E_x/\partial x + \partial E_z/\partial z = 0 \ . \qquad (68b)$$

This equation of constraint is easily solved for a plane wave since

$$E_x = E_0 \exp(\mathrm{i}kz) \qquad (69)$$

and there is no z component of $\mathbf{E}$.

But now consider an on-axis x-polarized freely diffracting Gaussian beam whose x component is

$$E_x = DE_0 \exp(\mathrm{i}kz) \exp[-(x^2+y^2)/w_0^2] \ . \qquad (70)$$

The partial derivative of $\partial E_x/\partial x$ is nonzero because of the transverse falloff of the beam. So there must be a nonzero z component of $\mathbf{E}$ with a nonzero z-derivative so as to satisfy the constraint equation of Eq.(68b). Since the fastest longitudinal variation of E_z is expected to be that of the exp(ikz) propagation factor, one has

$$E_z \approx \mathrm{i}k \ \partial E_x/\partial x \ . \qquad (71)$$

This correction field, to lowest order in s, is identical to the z component of $\mathbf{E}^{\mathbf{Davis}}$ of Eq.(64a). Substituting this into Eqs.(54a)-(54d) along with the circular-symmetry-preserving first term of the Taylor series expansion of exp[ε ($k\rho$) cos(φ-φ_0)] of Eq.(53) and using the van de Hulst localization principle, one obtains the correction term of the beam shape coefficients

$$A_n^0 = 2\mathrm{i} \ (n+1/2) \ \varepsilon\pi \cos(\varphi_0) \qquad (72a)$$

$$B_n^0 = 2\mathrm{i} \ (n+1/2) \ \varepsilon\pi \sin(\varphi_0) \ . \qquad (72b)$$

These are the same size as the m=0,2 corrections to the beam shape coefficients of Eqs.(58a)-(58d) due to circular symmetry breaking and described in Sec.4d. The results for a y-polarized beam and their comparison to Eqs.(59a)-(59d) is similar. Thus a nonzero $S_{VH}(\theta)$ and $S_{HV}(\theta)$ is due to a combination of the wave scattering effects of (i) circular symmetry breaking of the off-axis beam (i.e. the second term of Eq.(53) along with E_x and B_y), and (ii) the constraint that the off-axis incident beam must be a solution of Maxwell's equations (i.e. the first term of Eq.(53) with E_z and B_z). In the context of a Davis beam, these are the only two contributions to the beam fields of order ε. So it would seem that this exhausts the list of physical mechanisms responsible for the leading term of a nonzero $S_{VH}(\theta)$ and $S_{HV}(\theta)$.

5. Summary

Since cross-polarized scattering does not occur when an electromagnetic plane wave is scattered by a single homogeneous spherical particle, it has often been implicitly assumed that it continues to be impossible for all beams incident on the particle. But since a diagonally incident plane wave gives rise to both co-polarized and cross-polarized scattering, and complicated beams may be expressed as an angular spectrum of plane waves, it should happen in some cases that the cross-polarized components will not completely cancel out when integrated over the angular spectrum. When examining scattering by the localized model of a focused Gaussian beam we found that cross-polarized scattering does not occur for an on-axis focused Gaussian beam and a Gaussian beam translated off-axis in the scattering plane, but that cross-polarized scattering does occur for a Gaussian beam translated off-axis out of the scattering plane. We also found that for the beam and particle parameters examined here, it is orders of magnitude weaker than the intensity for co-polarized scattering. In this regard, it should be mentioned that we preliminarily experimented with varying the values of ρ_0 and w_0 by a factor of two from the values given in Fig.4 for VV and VH scattering with φ_0=180° and found that the ratio of the VH intensity to the VV intensity was slowly varying in this parameter range. In addition, a few results for varying φ_0 with fixed ρ_0 and w_0 are shown in Figs.5,6 of [12] and are interpreted there. Since the cross-polarized intensity depends on the scattering angle θ, as well as on the particle radius and refractive index, the beam width, and the off–axis beam location (ρ_0, φ_0), a systematic search of this extensive parameter space should hopefully be able to identify favorable conditions under which the strength of cross-polarized scattering is optimized and might be experimentally observed.

On a more theoretical note, we also found that when the beam first begins to be translated off-axis, the m=0,±2 azimuthal modes are the first to join the m=±1 modes of on-axis scattering, and produce the beginnings of the cross-polarized response of the sphere. An approximation to the exact GLMT scattering amplitudes is pursued in [12] which allows the sum over azimuthal modes m to be evaluated analytically, greatly decreasing the computer run time required for off-axis GLMT computations for scattering by particles with $a \gg \lambda$. Finally the role of diffraction, the Debye series decomposition of the partial wave scattering amplitudes, and time-domain scattering will be studied in [44].

Acknowledgement
J.A.L. and P.L. thank Prof. David Cannell of the University of California at Santa Barbara for a series of conversations that led to our investigation of cross-polarized scattering.

References

[1] Stein RS, Rhodes MB. Photographic light scattering of polyethylene films. J Appl Phys 1960; 31: 1873-85.
[2] Kerker M. The scattering of light and other electromagnetic radiation. New York:Academic;1969.
[3] Berne BJ, Pecora R. Dynamic light scattering. New York:Wiley-Interscience;1976.
[4] Asano A, Yamamoto G. Light scattering by a spheroidal particle. Appl Opt 1975; 14: 29-49, errata Appl Opt 1976; 15: 2028.
[5] Lock JA. Ray scattering by an arbitrarily oriented spheroid. II. Transmission and cross-polarization effects. Appl Opt 1996; 35: 515-31.
[6] Lock JA. Electric field autocorrelation functions for beginning multiple Rayleigh scattering. Appl Opt 2001; 40: 4187-4203.
[7] van de Hulst H.C. Light Scattering by Small Particles. New York:Dover;1981.
[8] Bohren CF, Huffman DR. Absorption and scattering of light by small particles. New York:Wiley-Interscience;1983.
[9] Mishchenko MI, Travis LD, Lacis AA. Scattering, absorption, and emission of light by small particles. Cambridge UK:Cambridge U. Press;2002.
[10] Goodman J. Introduction to Fourier Optics. San Francisco:McGraw-Hill;1968.
[11] Dociu A, Wriedt T. Plane wave spectrum of electromagnetic beams. Opt Comm 1997;136: 114-24.
[12] Lock JA, Laven P. Co-polarized and cross-polarized scattering of an off-axis focused Gaussian beam by a spherical particle. 2. Summation over azimuthal modes. JQSRT 2018; 221: 273-285.
[13] Lock JA. Contribution of high-order rainbows to the scattering of a Gaussian laser beam by a spherical particle. J Opt Soc Am A 1993;10:693-706.
[14] Lock JA. Improved Gaussian-beam scattering algorithm, Appl Opt 1995; 34: 559-70.
[15] Arfken G. Mathematical methods for physicists, third ed. Orlando FL:Academic;1985.
[16] Gouesbet G, Maheu B, Gréhan G. Light scattering from a sphere arbitrarily located in a Gaussian beam, using a Bromwich formulation. J Opt Soc Am 1988; 5: 1427-43.
[17] Gouesbet G, Gréhan G. Generalized Lorenz-Mie theories, second ed. Berlin:Springer International Publishing;2017.
[18] Wang JJ, Gouesbet G. Note on the use of localized beam models for light scattering theories in spherical coordinates. Appl Opt 2012;51:3832-6.
[19] Gouesbet G, Gréhan G, Maheu B. Localized interpretation to compute all the coefficients g_n^m in the generalized Lorenz-Mie theory, J Opt Soc Am A 1990:7;998-1007.
[20] Gouesbet G, Lock JA. Rigorous justification of the localized approximation to the beam-shape coefficients in generalized Lorenz-Mie theory. II. Off-axis beams. J Opt Soc Am A 1994; 11: 2516-25.
[21] Lock JA. Angular spectrum and localized model of Davis-type beam. J Opt Soc Am A 2013; 30: 489-500.
[22] Gouesbet G, Lock JA, Gréhan G. Generalized Lorenz-Mie theories and description of electromagnetic arbitrary shaped beams: Localized approximations and localized beam models, a review. JQSRT 2011; 112: 1-27.

Published in Journal of Quantitative Spectroscopy and Radiative Transfer 221 (2018) 260 - 272

[23] Gouesbet G, Lock JA. Comments on localized and integral localized approximations in spherical coordinates. JQSRT 2016; 179: 132-6.
[24] Lock JA, Gouesbet G. Rigorous justification of the localized approximation to the beam-shape coefficients in generalized Lorenz-Mie theory. I. On-axis beams. J Opt Soc Am A 1994; 11: 2503-15.
[25] Gréhan G, Maheu B, Gouesbet G. Scattering of laser beams by Mie scatter centers: numerical results using a localized approximation. Appl Opt 1986;25: 3539-48.
[26] Xaiowei J, Shen J, Yu H. Calculation of generalized Lorenz-Mie theory based on the localized beam models. JQSRT 2017; 195: 44-54.
[27] Qiu J, Shen J. Beam shape coefficient calculation for a Gaussian beam: localized approximation, quadrature and angular spectrum decomposition methods. Appl Opt 2018;57:302-13.
[28] Shen J, Jia X, Yu H. Compact formulation of the beam shape coefficients for elliptical Gaussian beam based on localized approximation. J Opt Soc Am A 2016;33:2256-63.
[29] Shen J, Liu X, Wang W, Yu H. Calculation of light scattering of an elliptical Gaussian beam by a spherical particle. J Opt Soc Am A 2018;35:1288-98.
[30] Maheu B, Gréhan G, Gouesbet G. Generalized Lorenz-Mie theory: first exact values and comparisons with the localized approximation. Appl Opt 1987;26:23-5.
[31] Maheu B, Gréhan G, Gouesbet G. Ray localization in Gaussian beams. Opt Comm 1989;70:259-62.
[32] Gouesbet G, Wang JJ, Han YP. Transformations of spherical beam shape coefficients in generalized Lorenz-Mie theories through rotation of coordinate system. I. General formulation. Opt Comm 2010;283:3218-25.
[33] Gouesbet G, Lock JA, Wang JJ, Gréhan G. Transformations of spherical beam shape coefficients in generalized Lorenz-Mie theories through rotation of coordinate system. V. Localized beam models. Opt Comm 2011;284:411-7.
[34] Ren KF, Gréhan G, Gouesbet G. Symmetry relations in generalized Lorenz-Mie theory. J Opt Soc Am A 1994;11:1812-7.
[35] Langley DS, Marston PL. Glory in optical backscattering from air bubbles. Phys Rev 1981;47:913-6.
[36] Marston PL, Langley DS. Glory in backscattering: Mie and model predictions for bubbles and conditions on refractive index in drops. J Opt Soc Am A 1982;72:456-9.
[37] Marston PL. Uniform Mie-theoretic analysis of polarized and cross-polarized optical glories. J Opt Soc Am 1983;73:1816-8.
[38] Laven P. Scattering of Gaussian beams by a spherical particle. http://www.philiplaven.com/p3d2.html.
[39] Konnen GP, de Boer JH. Polarized rainbow. Appl Opt 1979;18:1961-5.
[40] Lock JA, Laven P. The Debye series and its use in time-domain scattering, in Kokhanovsky A. ed. Light Scattering Reviews 11. Springer Praxis: Berlin;2016.
[41] Merzbacher, E. Quantum Mechanics, second ed. New York:Wiley;1970.
[42] Davis LW. Theory of electromagnetic beams. Phys Rev A 1979;19:1777-79.
[43] Barton JP, Alexander DR. Fifth-order corrected electromagnetic field components for a fundamental Gaussian beam. J Appl Phys 1989;66:2800-2802.
[44] Laven P, Lock JA. Co-polarized and cross-polarized scattering of an off-axis focused Gaussian beam by a spherical particle. 3. Diffraction, the Debye series, and time-domain scattering. JQSRT 2018; 221, 286-299.